Published in IET Communications
Received on 30th September 2011
Revised on 3rd February 2012
doi: 10.1049/iet-com.2011.0707

In Special Issue on Energy Aware Wireless Network Protocols

ISSN 1751-8628

Energy-efficient and reliable multicasting for WiMAX multi-hop relay networks

C.-Y. Chen[1] *W.-K. Jia*[1,2] *Y.-C. Chen*[1]

[1]*Department of Computer Science, National Chiao Tung University, Hsinchu, Taiwan*
[2]*Department of Advanced Research Institute (ARI), Institute for Information Industry (III), Taipei, Taiwan*
E-mail: chiayao@cs.nctu.edu.tw

Abstract: Orthogonal frequency division multiplexing (OFDM)-based wireless transmission technologies such as WiMAX are now widely deployed, and the frame check sequence (FCS) scheme is used to enhance the reliability of OFDM-based systems. As the padding overhead cannot be completely avoided in such systems when variable-length medium access control (MAC) frames are encapsulated, the authors propose a novel cyclic redundancy check (CRC)-based error-correction scheme that utilises the frame padding overhead to carry as much extra segmented FCS information as possible. In a multi-hop relay environment, a mobile station might receive a multicast frame more than once, so the error bit correction scheme could be triggered in the first transmission. In the IEEE's work, the original CRC scheme is optional and only has limited error-detection capability in upper MAC layer. FCS requires a few bits in a frame, but in our work, CRC is compulsory and all sub-FCSs are carried by padding space without using any extra bit. For the best error-correction capability, all transmissions must be padded as many sub-FCSs are possible in cross layer. The proposed approach achieves a significant performance improvement over the legacy FCS scheme in terms of error detection and correction of multicast frames in a transparent mode multi-hop relay network, and it is redundancy-free as well as energy efficient. The authors assess the performance improvement via both mathematical analysis and simulations. The results show that the mobile stations get significant improvement of goodput and utilisation in an error-prone WiMAX multi-hop relay network.

1 Introduction

Orthogonal frequency division multiplexing (OFDM)-based wireless networks such as WiMAX are now widely deployed. As data transfer under OFDM modulation occurs in an error-prone wireless environment, some data may be corrupted by the inevitable interference (e.g. path-loss, fading, shadowing and attenuation) inherent in such environments [1–3]. Hence, error control schemes must be deployed to ensure that OFDM-based wireless networks are reliable. There are two major error control schemes, namely, the automatic repeat request (ARQ) mechanism and the hybrid ARQ (HARQ) mechanism, which are deployed in the logical link control sublayer of medium access control (MAC) layer and the physical layer, respectively.

In an ARQ scheme, the error-detection mechanism is activated by both the sender and the receiver to check whether the received data frame has been corrupted during the transmission. If the receiver detects an error, it will notify the sender by transmitting a Negative ACKnowledgement signal, and the sender will retransmit the data within a certain period of time. In a HARQ scheme, both error detection and error correction are utilised to recover corrupted data. If the receiver fails to recover the corrupted data, a retransmission process, such as ARQ, will be executed.

Normally, error-detection schemes and error-correction schemes are implemented independently. The most popular error-detection scheme, cyclic redundancy check (CRC), is usually appended to a data frame. Owing to the limited information carried in the CRC field, the receiver is unable to correct and retrieve a corrupted frame, which will then be dropped automatically. To provide reliable data transfer over an error-prone communication link, CRC schemes usually cooperate with the forward error-correction (FEC) mechanism and/or ARQ mechanism. FEC does not introduce a delay factor, but it leads to lower throughput because of redundancy in the data frame [1, 3]. ARQ, on the other hand, causes long delays because it uses retransmission to deal with channel errors. [2–7]. In theory, an OFDM data-burst comprised a set of OFDM-based symbols should leave a certain amount of padding space when variable-length MAC frames are included in the OFDM burst [1, 5]. In addition, a corrupted frame still contains useful information that could help the receiver derive the data in the original frame in case the retransmission process fails again.

The multicast/broadcast service (MBS) feature of mobile network is a promising technology for providing wireless multimedia service, because it allows the delivery of multimedia content to large-scale user communities in a cost-effective manner. Using MBS, a certain part within each superframe can be set aside for multicast-only or broadcast-only data, as shown in Fig. 1. The entire frame can also be designated as a downlink-only broadcast frame. A major task of the MBS module is to provide a reliable

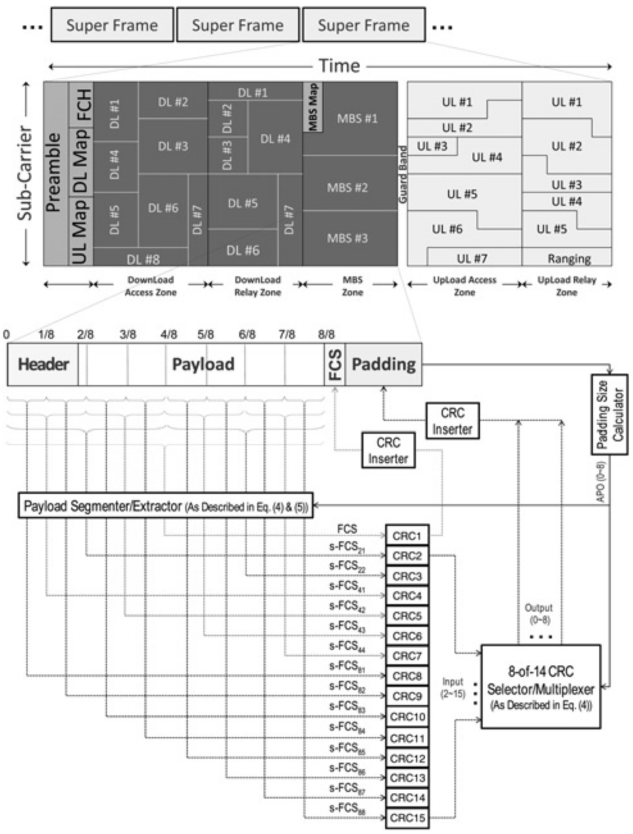

Fig. 1 *WiMAX MR frame structure and function diagram used in the proposed scheme*

sequence of MBS frames to multiple recipients simultaneously. Thus, the data transfer might continue until all data are transferred to all of the intended receivers, resulting in a potentially unlimited duration for an individual MBS stream.

Further, for mobile receivers, energy savings are one of the major concerns. As the reliability of the wireless link is generally based on the retransmission strategy in which unsuccessful transmissions are repeated a certain number of times. Thus the mechanism must consider that the receiver devices have limited energy capacity which may cause significant power consumption because of frequent retransmissions. In order to minimise the power consumption of the MAC protocols, it is useful to avoid persistence in retransmitting data, to tradeoff number of retransmission attempts for probability of successful transmissions, and to inhibit transmission when channel conditions are poor.

On the other hand, to improve the throughput and coverage of the original single-hop systems [4], the 802.16j standard [8] defines two operating modes: (i) the transparent mode and (ii) the non-transparent mode. The key difference between these two relay modes lies in how they transmit the frame information: the relay station (RS) transmits the frame header information in the non-transparent mode, but not in the transparent mode. The frame header contains essential information that the nodes use to determine when they can transmit and receive information. Theoretically, in the transparent mode, the mobile station (MS) within a RS's coverage will receive a multicast frame at least twice, from the RS and from the base station (BS). However, they do not have enough information to handle frames sent by the BS.

In this paper, we focus on the issues that arise in 802.16j systems, such as how relays operate in the transparent mode. We propose a novel CRC-based error-correction scheme for multicasting in transparent mode multi-hop relay (MR) networks. The scheme performs multiple checks to ensure the accuracy of received data; hence, it reduces the frequency of retransmissions. Our key objective is to fully utilise the padding in order to extend the original CRC information. Besides the original frame check sequence (FCS), we subdivide the entire payload into several independent data blocks and calculate the FCS of each one. The sub-FCS blocks are then inserted into the original padding position until the padding space is full. Under our approach, if an error occurs in a received frame, the receiver can initially detect the error by checking the original FCS. If the frame contains extra sub-FCS blocks, the receiver can determine exactly which sub-block is corrupted. Furthermore, we can combine two corrupted frames to derive the correct frame based on the corresponding correct sub-blocks.

The rest of the paper is organised as follows. The background and related works are described in Section 2. In Section 3, the proposed scheme is discussed in details. In Section 4, simulation and number results are presented for performance evaluation. Section 5 concludes the work.

2 Conventional ARQ and error-detection scheme

In conventional ARQ schemes, error-detection information (e.g. parity-check and checksum information) is added to the existing data frame for transmission. The error-detection scheme directly affects the transmission efficiency of communication networks. The CRC scheme is a powerful class of coding scheme, especially for the detection of random errors and even burst errors in a poor-quality communication link. The CRC scheme is widely used in both wireless and wired networks [1–3, 9], and it is particularly well suited for the speedy detection of erroneous frames in the MAC layer. Detailed information about the scheme can be found in [10, 11].

CRC uses a polynomial-modulo-operation with a generator polynomial $g(x)$, which is a binary polynomial with degree r, to calculate the FCS of the binary net data (ND) [10] with the following equation

$$\text{fcs}(x) = (\text{nd}(x) \times x^r) \bmod g(x) \tag{1}$$

where nd(x) and fcs(x) denote the polynomial counterpart of ND and FCS, respectively. The length of FCS is r, which is the degree of $g(x)$. A telegram $T = [\text{ND}, \text{FCS}]$ is transmitted to the receiver, which only receives data if (2) holds. The received data is labelled with an apostrophe to indicate that it might have been corrupted during transmission.

$$t'(x) \bmod g(x) = ((\text{nd}'(x) \times x^r) + \text{fcs}(x)) \bmod g(x) = 0 \tag{2}$$

Calculating the FCS at the sender or checking it at the receiver is realised by a linear feedback shift register or a corresponding table look-up method. If the sender and receiver need to calculate or check multiple FCS simultaneously, the computation cost will increase. For this reason, the CRC mechanism is usually implemented in the hardware circuit to eliminate the possibility of computing latency.

IET Commun., 2012, Vol. 6, Iss. 14, pp. 2169–2177
doi: 10.1049/iet-com.2011.0707

3 Proposed scheme

3.1 OFDM encapsulation and padding in WiMAX systems

We now consider the problem of data-burst grooming in OFDM-based networks. In such networks, frames with the same edge-node destination are assembled in a transmission unit called a data burst (a.k.a. data region) [4, 5], which is a two-dimensional allocation of contiguous logical sub-channels in a group of contiguous OFDM symbols (or slots). Sub-channels may be allocated on the OFDM downlink by partial usage of sub-channels (PUSC) or full usage of sub-channels (FUSC). For downlink FUSC and downlink optional FUSC using the distributed subcarrier permutation, one slot is a sub-channel with one OFDM symbol. For downlink PUSC using the distributed subcarrier permutation, one slot is a sub-channel with two OFDM symbols. This allocation may be visualised as a rectangle, such as a 4×8 rectangle. MAC frames should be processed and mapped to an OFDM data burst for downlink and uplink transmission by using the respective algorithms. Data bursts have a minimum length, which is based on the sub-channel allocation mode. In other words, the encapsulation process is likely to leave a little surplus padding space when MAC frames are added to the rectangle [4, 5]. The above panel in the Fig. 1 shows the downlink sub-frame structures.

Furthermore, modulation and coding schemes (MCS) are critical factors that affect the growth of the padding overhead. For example, in IEEE 802.16 WiMAX systems, which support various MCS, binary phase shift keying (BPSK), 16 and 64 quadrature amplitude modulation (QAM) are mandatory on the downlink for WiMAX; whereas 64 QAM is optional on the uplink. In an OFDM-based system, for both variable-length frames and fixed-length frames, a data burst's padding overhead varies according to the type of sub-frame, the modulation and coding scheme, the resource allocation scheme, and the frame-length distribution. In general, the smaller the number of OFDM symbols in a burst, the larger will be the padding overhead. According to work in [1, 12, 13], the overhead to payload ratio may be more than 30% depending on the frame-length distribution, modulation rate, coding rate and burst length. In a simulation environment, the maximum possible padding overhead would be 4.3%, assuming a frame length of 1518 bytes with a 64 QAM 3/4 modulation and coding rate. Excessive padding usually results in inefficiency and a high data-burst-blocking probability.

Several methods have been proposed to reduce the padding overhead in OFDM-based systems [12, 13]. Unlike previous approaches, our method does not attempt to reduce the padding overhead. Instead, it tries to fully exploit the overhead to (i) create a robust OFDM-based error-detection/correction scheme; and (ii) construct a highly efficient OFDM-based transmission system that significantly reduces the retransmission rate in an environment with extremely poor radio quality.

3.2 MBS in WiMAX MR networks

IEEE 802.16j MR [8, 14, 15] systems generate a great deal of interest because they have the potential to achieve cost savings while increasing the coverage and/or capacity of IEEE 802.16e-2005 networks [4]. The transparent mode RS does not forward frame information, but simply forward data for the BS and its MS; therefore it does not extend the coverage of the BS. In the transparent mode, the path between the BS and the MS is at most two hops, and only one RS can participate in relaying packets between the BS and the MS. The main objective of deploying RSs in the network is to increase the network capacity within the BS coverage area, rather than increase the size of that area. In this environment, when the BS sends a multicast frame, some MSs in the overlapping area between the BS and the RS coverage will receive the same frame twice, that is, from the BS and from the RS; however, the MSs do not have enough channel information to handle the frame from the BS.

In [8], the network entry procedure involves three steps: admission control, adjustment of the local transmission parameters and topology discovery. In the transparent mode, the BS must determine whether the MS is attached directly to it or through the best RS. Normally, only one path will be selected. To make error correction more efficient when the MS attaches to an RS under the proposed scheme, the BS always chooses two paths to the MS (from both the RS and the BS). The response message will include details of the two paths to the MS. Fig. 2 shows the multicast service based on our scheme in a MR network. All RSs are placed on the boundary of the BS 16 QAM coverage area with radius $R2$, and they rebroadcast designated traffic to MSs within different modulation coverage radiuses $r1 - r3$. For example, when the MS is located in zone 1, it attaches to the BS directly and also receives the high-modulation order (e.g. 64 QAM) frames from the BS directly. However, the MS located in zone 6 will receive a middle-modulation order (e.g. 16 QAM) frame from the RS indirectly and a low-modulation order (e.g. BPSK) frame from the BS directly.

3.3 Padding-based extra-CRC error-correction scheme

In this section, we consider the error-correction scheme for the transmission side (BS), receiver side (MS) and relay side (RS) of a network. Under the scheme, the RS forwards multicast frames normally, that is, in the same way as the original relay network does.

3.3.1 Base station: Before a frame is transmitted, the BS needs to decide the padding length and padding content.

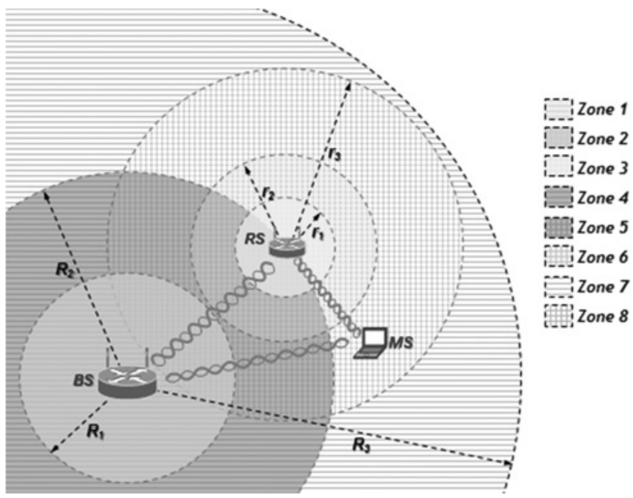

Fig. 2 *Multicast service in WiMAX MR network*

The padding length of frame in ith transmission can be denoted as Z_i. Unlike the original padding method, the s-FCSs are used as the padding content. Based on the average padding overhead, a BS can choose the padding content immediately, and the average padding overhead p_o can be calculated using the following equation

$$p_o = \left\lfloor \frac{Z_i}{r} \right\rfloor \quad (3)$$

where r denotes the length of the FCS. The sequence $O_k - \langle O_0, O_1, O_2 \ldots O_{p_o-1} \rangle$ indicates that the offset location of the payload is

$$\underset{k=0,1,2\ldots p_o-1}{O_k} = \begin{cases} k/2^{\lfloor \log_2 p_o \rfloor} & \text{if} \quad k < 2(p_o - 2^{\lceil \log_2 p_o \rceil}) \\ k - (p_o - 2^{\lceil \log_2 p_o \rceil})/2^{\lceil \log_2 p_o \rceil} & \text{if} \quad k \geq 2(p_o - 2^{\lceil \log_2 p_o \rceil}) \end{cases} \quad (4)$$

The sequence $S_k - \langle S_0, S_1, S_2 \ldots S_{p_o-1} \rangle$ shows that the size of a separate payload is

$$\underset{k=0,1,2\ldots p_o-1}{S_k} = \begin{cases} 1/2^{\lfloor \log_2 p_o \rfloor} & \text{if} \quad k < 2(p_o - 2^{\lceil \log_2 p_o \rceil}) \\ 1/2^{\lceil \log_2 p_o \rceil} & \text{if} \quad k \geq 2(p_o - 2^{\lceil \log_2 p_o \rceil}) \end{cases} \quad (5)$$

The BS can use O_k and S_k simultaneously to calculate extra sub-FCSs while constructing a frame. The length of all s-FCSs is equal to the length of the FCS. In the example shown in Fig. 1, the BS derives the FCS and 14 extra s-FCSs (CRC_2–CRC_{15}), and selects the required number of s-FCSs to pad the frame according to the padding length.

3.3.2 Mobile station: In a MR network environment, a MS may attach to a BS directly or through an RS. In the former scenario, when a multicast frame arrives, the MS checks the FCS and all the s-FCSs simultaneously. If the frame passes the FCS check, it means the received ND has no corruption. In case that the FCS fails the check, but all the s-FCSs pass it, then only the FCS is corrupted and the ND is correct. In these two cases, it is not necessary to retransmit the frame. However, if the FCS or any s-FCS fails the check, the frame must be retransmitted, and the MS must record the correct data blocks that already passed the s-FCS check. The check procedure is the same for the second type of transmission, that is, via an RS. If any s-FCS fails the check in the second type of transmission, the MS can use the 'correct data block information' of any two transmissions via the RS or BS to correct the ND. Although the FCS and some s-FCSs fail the check in the second type of transmission, the MS can obtain the correct ND by using the record of correct data blocks.

If an MS attaches to an RS, it will receive a frame twice. The MS can perform the FCS check twice in one transmission and will probably be able to correct an error in that transmission by using the record of correct data blocks. However, if the MS checks the two frames and finds that the ND is still corrupted, the frame must be retransmitted. Fig. 3 shows the error-correction procedure in a MR network.

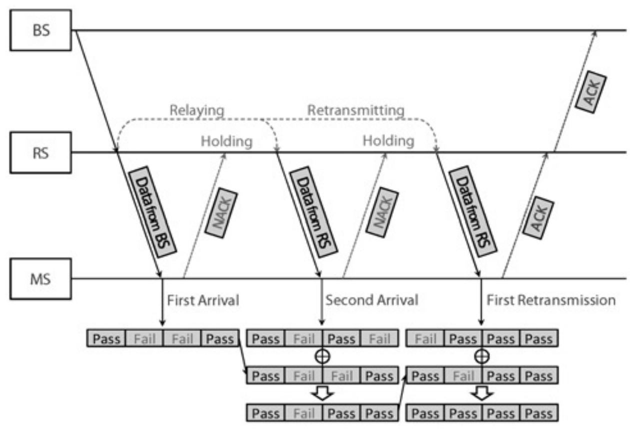

Fig. 3 *Error-correction procedure in a WiMAX MR network*

3.3.3 Relay station: In the proposed scheme, the RSs forward multicast frames in the same way as RSs in the original relay network environment; and they execute the new error-correction method like an MS attached to the BS directly.

4 Performance evaluation

4.1 Simulation scenarios

Fig. 2 also depicts the simulation topology. In this simple example, six RSs at distance R_2 (described in previous section) from the BS form a 60° with the BS axis. Each RS covers a primary target zone, note that zones overlap each other to provide redundancy between two adjacent RSs. The MSs are randomly dropped with a uniform distribution in the BS's coverage area. A video server is connected to a BS with high-speed wired link; multicast streaming requests are randomly generated from each MS in the network. The network parameters used to evaluate the performance of the proposed error-correction scheme are summarised in Table 1 [16–20]. We assume that the BS, RSs and MSs always use the lower modulation rate in order to achieve a larger coverage. Only one BS is used in transparent mode relay networks. The deployment of RSs considered in this paper includes hexagonal cells regrouped into clusters in which the frequency channels are unique. It is also assumed that the coverage area of each cell is free of holes. To achieve the best relay performance, all RSs are located on the boundary of BS 16 QAM MCS. The distance between the BS and each RS is 4.1 km; and the distance between the RSs on the boundary is also 4.1 km.

The cell coverage in transparent mode relay networks is the same as the BS BPSK coverage. In this scenario, the maximum transmission range of the BS is 7.7 km. The

Table 1 Parameters

Parameter	Value
transmission power of BS	30 dBm
transmission power of RS	23 dBm
sub-channel bandwidth	20 MHz
channel frequency	5.47 GHz
thermal noise	−100, 97 dBm
CRC type	CRC-16
length of FCS	16 bits
length of ND	1024 bits

IET Commun., 2012, Vol. 6, Iss. 14, pp. 2169–2177
doi: 10.1049/iet-com.2011.0707

MCS for all links in the cell is evaluated to determine the impact of the proposed CRC-based error-correction scheme. When an MS locates in the same MCS level of the BS and RS, it can attach to (i) the BS first or (ii) the RS first. The first strategy has the shortest latency, and the second one yields the best error-correction performance. Table 2 details the zone type and coverage for each type of link in a cell under two attachment strategies.

4.2 Padding length

The padding length Z_i of frame in ith transmission can be calculated from the burst size and the amount of data in the burst. Let Γ_i denote the burst size and E_i denote the datagram size of frame in ith transmission (including the frame header), the size Γ_i of an OFDM burst will be greater than or equal to E_i because the burst size includes the data size and the padding length (see Fig. 2). Z_i can be calculated as follows

$$Z_i = \begin{cases} \Gamma_i - E_i, & \text{if } \Gamma_i > E_i \\ 0, & \text{if } \Gamma_i = E_i \end{cases} \tag{6}$$

where $\Gamma_i = \left((\theta \times N_s) \times S_c \times \frac{(M \times C_r)}{8}\right)$

In (6), θ denotes the number of data subcarriers, N_s denotes the number of symbols in a frame, S_c denotes the number of subcarriers, M is the M-QAM alphabet size, and C_r is the coding rate of the modulation. Fig. 4 shows the padding length in different modulation orders when the packets in any length-distribution (traffic pattern) are encapsulated in fitted OFDM bursts. All types of frames must contain variable-length padding, and high-order modulations will have more padding than low-order modulations. We setup a simulation based on six input traffic patterns (uniform distribution, standard normal distribution, U distribution, left-skewed distribution, right-skewed distribution and the statistical characteristic of real traffic patterns) to estimate the average padding lengths. In Fig. 4, the average padding lengths in BPSK/QPSK, 16 QAM and 64 QAM are 4–8 bytes, 8–15 bytes and 15–22 bytes. Based on these results, we set the average padding overhead p_o of BPSK, 16 QAM and 64 QAM at 2, 4 and 8, respectively, in the simulation.

Table 2 Zone type and its coverage

Zone	Coverage	Attachment strategy, %	
		BS first	RS first
zone 1	BS: 64 QAM only	8.16	8.16
zone 2	BS: 16 QAM, RS: 64 QAM	4.39	4.39
zone 3	BS: BPSK, RS: 64 QAM	5.45	5.45
zone 4	BS: 16 QAM only	15.52	6.07
zone 5	BS: 16 QAM, RS: 16 QAM	–	9.45
zone 6	BS: BPSK, RS: 16 QAM	13.22	13.22
zone 7	BS: BPSK only	53.26	15.1
zone 8	BS: BPSK, RS: BPSK	–	38.16

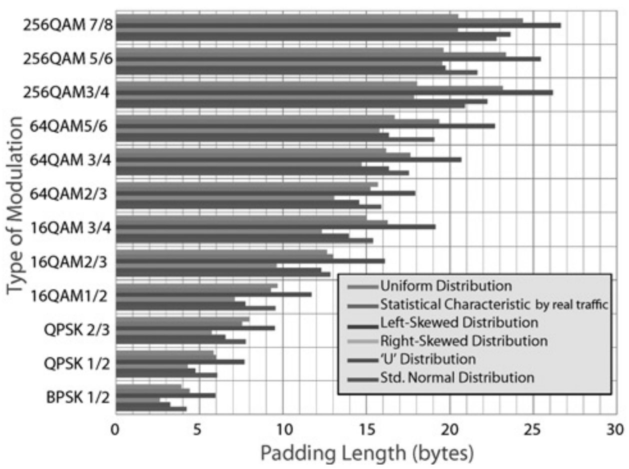

Fig. 4 *Modulation order against padding size with various traffic patterns*

4.3 Radio propagation and interference model

In a production network, the signal quality between a sender and a receiver is attenuated because of number of factors, such as the shadowing, fading and path loss. Those factors, along with interference at the receivers, are critical features of any model of a wireless system. In the following, we describe the radio and interference models used in this work.

Our radio propagation model only considers attenuation caused by path loss because of signal propagation over a long distance. The fading and shadowing effects are not considered. In the model, which is based on the Stanford University Interim path loss model recommended by the 802.16 task group [14], some assumptions about the sender's power and antenna gains can be used to determine the power of the signal received at MS as well as the signal-to-noise ratio (SNR). By mapping the receiver's SNR to one of the thresholds specified in [4], the MCS to be used between the communicating nodes can be determined. The SNR at the receiver is calculated as follows

$$\text{SNR}_{[\text{dB}]} = 10\log_{10}\left(\frac{\tilde{p}_{\text{MS}}}{\text{BW}N_o}\right) \tag{7}$$

where BW denotes the effective channel bandwidth in Hz; N_o is the thermal noise density; and $\tilde{p}_{\text{MS}}$ is the power of the signal received at the MS, and can be derived as follows

$$\tilde{p}_{\text{MS}} = \frac{G_{\text{BS}} G_{\text{MS}} P_{\text{BS}}}{L(\text{BS, MS})} \tag{8}$$

where P_{BS} is the transmission power of the BS; G_{BS} and G_{MS} are the antenna gains at the BS and MS, respectively, and L(BS, MS) is the path loss from the BS to MS. Given the SNR of the MS, the BS can determine the MCS based on Table 3. Specifically, the BS will use the highest MCS whose minimum required SNR is smaller than SNR$_{[\text{dB}]}$.

Table 3 MSC and SNR threshold

MSC	Threshold α, dB
BPSK 1/2	6
BPSK 3/4	9
16 QAM 1/2	11.5
16 QAM 3/4	15
64 QAM 1/2	17
64 QAM 2/3	19
64 QAM 3/4	21

The distance between the BS and the MS is dependent of the signal power and the noise, and can be calculated as follows [16]:

$$d = \frac{\lambda \times 10^{(p_t[\mathrm{dB\,m}] - \mathrm{SNR[dB]} - N[\mathrm{dBm}]/20)}}{4\pi} \quad (9)$$

In (9), λ denotes the wavelength, p_t denotes the transmission power and N denotes the noise. Equation (9) can be rewritten as follows

$$\mathrm{SNR}_{[dB]} = p_{t[dBm]} - N_{[dBm]} - 20\log\frac{4\pi d}{\lambda} \quad (10)$$

Using (10), the SNR can be estimated when MS locates in different positions.

4.4 Packet error rate

The bit error probability (BEP) of various types of modulation can be derived by using the SNR. In the case of multilevel-QAM, the BEP, P_b can be approximated as follows

$$P_b \cong \frac{4}{\log_2 M}\left[1 - \frac{1}{\sqrt{M}}\right] Q\left(\sqrt{\left[\frac{3}{M-1}\right]\frac{E_b}{N_0}}\right) \quad (11)$$

In (11), M denotes the M-QAM alphabet size. The packet error rate (PER) of the ith transmission, which uses the original CRC scheme, can be calculated as follows

$$\mathrm{PER} = [1 - (1 - P_b)^{m+r}]^i \quad (12)$$

In (12), m represents the length of ND, r is the length of the FCS and $(m + r)$ denotes the total length of the frame. In the proposed scheme, if an MS attaches to the BS, the double checking procedure can correct a corrupted FCS; hence, the PER of the ith transmission can be calculated as follows

$$\mathrm{PER} = [1 - (1 - P_b)^m]^i \times [1 - (1 - P_b)^{(m/p_o)}]^{i-1} \quad (13)$$

where p_o is the average padding overhead of the same data block in two consecutive transmissions. When an MS attaches to an RS, the PER of the ith transmission can be calculated as follows

$$\begin{aligned}\mathrm{PER} =& [[1 - (1 - P_{b1})^m] \times [1 - (1 - P_{b2})^m] \\ &\times [1 - (1 - P_{bx})^{(m/\min(p_{o1}, p_{o2}))}]]^i \end{aligned} \quad (14)$$

In (14), p_{o1} and p_{o2} are the average padding overheads of frames from the BS and RS, respectively, and P_{b1} and P_{b2} are the bit error probabilities of frames from the BS and RS, respectively. P_{bx} is the maximum of P_{b1} and P_{b2}.

Figs. 5*a* and *b* show the PERs of the original error-correction scheme in various locations. During the first transmission, the PER is higher than 50% in 93.38% of the area. It is lower than 20% in only 3.76% of the area. Although retransmission can reduce the PER, as shown in Fig. 5*b*, the effect is limited. After the second transmission, the PER is less than 20% in 5.8% of the area, and less than 50% in 9.7% of the area. Figs. 5*c*–*f* show that the PER of the proposed error-correction scheme for the ‘BS first’ and ‘RS first’ attachment strategies, respectively. Using the proposed error-correction scheme can effectively reduce PER in the first transmission. For example, in Fig. 5*c*, the PER in zones 2, 3 and 6

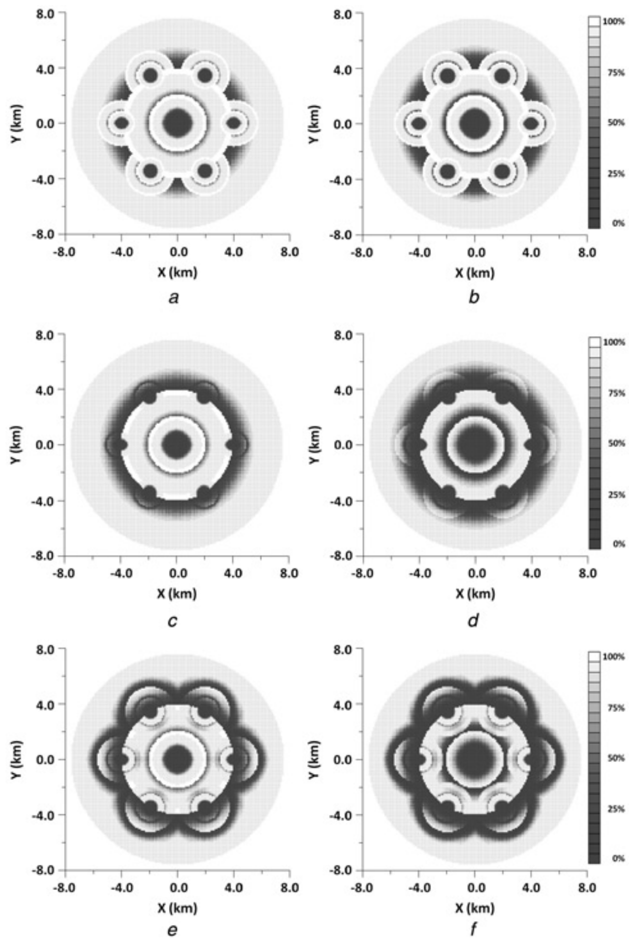

Fig. 5 *PER of the original error correction scheme in*
a First transmission
b Second transmission (first retransmission)
The proposed error-correction scheme using the ‘BS first’ strategy in the
c First transmission
d Second transmission (first retransmission)
The proposed error-correction scheme using the ‘RS first’ strategy in the
e First transmission
f Second transmission (first retransmission)

improves significantly. The PER is lower than 20% in 7.41% of the area, and lower than 50% in 14.22% of the area. The proposed scheme has a better error-correction capacity than retransmission, which uses the original CRC scheme. After retransmission, this uses the new scheme as shown in Fig. 5*d*, the PER is below 20% in 17.02% of the area and below 50% in more than 25% of the area. Although our scheme can correct bit errors during the first transmission in some zones, the impacted area of the BS first attachment strategy is too little (only 20.06 % coverage). Using the RS first strategy increases the impacted area to 70.67%, so the proposed error-correction scheme is more effective. The PER of the first transmission when the MS prefers to attach to the RS is shown in Fig. 5*e*. The area where the PER is lower than 20% rises to 13.28%, and the area where it is lower than 50% rises to 23.17%. However, after the second transmission, those areas increase to 23.34 and 32.6%, respectively, as shown in Fig. 5*f*. Table 4 shows the PER against the coverage under different schemes.

4.5 Actual transmitted data (packet delivery ratio)

The actual transmitted data (‘ATD’) is the size of the transmitted data, including the total frame and the

doi: 10.1049/iet-com.2011.0707

Table 4 PER against coverage

PER	Coverage					
	Original scheme, %		Proposed scheme with BS first strategy, %		Proposed scheme with RS first strategy, %	
	First TS	Second TS	First TS	Second TS	First TS	Second TS
0–20%	3.76	5.8	7.41	17.02	13.28	23.34
20–50%	2.41	3.9	6.81	8.93	9.89	9.26
50–100%	93.83	90.3	85.78	74.05	76.83	67.4

TS, transmission

retransmitted frame. The ATD will be no smaller than E_i. When the transmission uses the original CRC scheme, the ATD can be defined as follows

$$\text{ATD} = \frac{E_i}{(1-P_b)^{m+r}} \tag{15}$$

Under the proposed scheme, when an MS attaches to the BS directly, the ATD_{BS} of the transmission can be calculated as follows

$$\text{ATD}_{\text{BS}} = \frac{E_i(1+(1-P_b)^{((m)/(p_0))}-(1-P_b)^{((m)/(p_0))+m})}{(1-P_b)^m+(1-P_b)^{((m)/(p_0))}-(1-P_b)^{((m)/(p_0))+m}} \tag{16}$$

Similarly, when an MS attaches to an RS, the ATD_{RS} of the transmission can be calculated as follows:

$$\text{ATD}_{\text{RS}} = \frac{E_i}{1-\{[1-(1-P_{b1})^m]\times[1-(1-P_{b2})^m] \times[1-(1-P_{bx})^{(m/(\min(p_{o1},p_{o2})))}]\}} \tag{17}$$

Fig. 6 illustrates the relationship between the goodput and SNR of the BS in zones 1, 4 and 7, where the MS attaches to the BS directly. The size of the total amount of transmitted data divided by ATD equals the goodput. When the value of the goodput is 100%, it is equal to the total available bandwidth. In good transmission conditions, the performance of the proposed scheme is almost the same as that of the original scheme; however, under poor transmission conditions, the proposed scheme yields better goodput. The results in Figs. 6 and 7 demonstrate that, for all zones, the proposed error-correction scheme achieves a significant performance improvement over the original scheme. The larger the M-QAM alphabet size, the greater the improvement will be. In zone 1 (using 64 QAM), zone 4 (using 16 QAM) and zone 7 (using BPSK) the performance is enhanced by 1–2, 1 and 0.5 dB, respectively.

If the RS signal is strong, the goodput of proposed scheme is similar to that of the original scheme. For example, in Fig. 7*a*, when the SNR of the RS is 5 dB and the SNR of the BS is 24 dB, the goodput of the original scheme and the proposed scheme in zone 2 is 85.02 and 85.24%, respectively. With a weaker RS signal, the proposed scheme uses frames from the BS to enhance the error-correction rate; therefore it improves the goodput significantly. Fig. 7*a* also shows that when the SNR of the RS is 10 dB and the SNR of the BS is 22 dB, the goodput of original scheme in zone 2 is zero, but that of the proposed scheme is 100%. Similar trends are evident in the

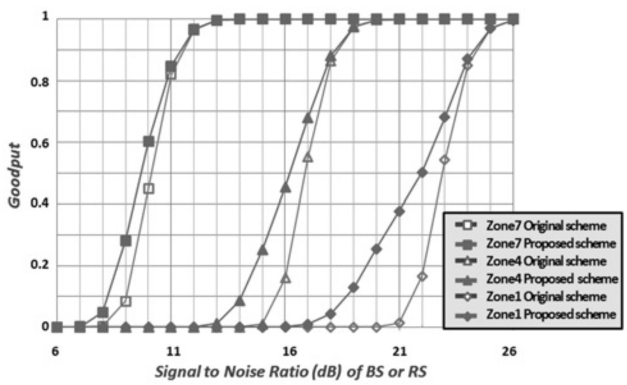

Fig. 6 *Goodput against SNR in zones 1, 4 and 7*

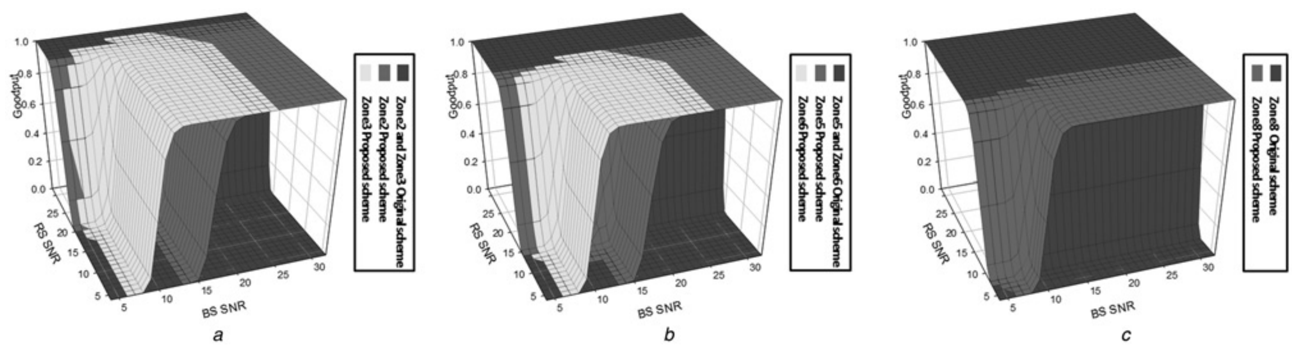

Fig. 7 *Goodput against SNR in*

a Zones 2 and 3
b Zones 5 and 6
c Zone 8

Table 5 Goodput integral in different zone

Zone type	Goodput integral, CDF		Enhancement, %
	Original scheme	Proposed scheme	
zone 1	41.13	67.1	63.14
zone 2	41.13	189.7	361.22
zone 3	41.13	308.89	651.01
zone 4	161.24	176.84	9.68
zone 5	161.24	261.2	61.99
zone 6	161.24	339.92	110.82
zone 7	296.42	304.94	2.87
zone 8	296.42	374.84	26.46

other zones, as shown in Figs. 7*b* and *c*. Table 5 shows the goodput integral (i.e. cumulative distribution function (CDF)) from SNR = 5 to 25 in different zone types. When using the proposed scheme, goodput in all zones are significantly improved. In particular, in zones where the MS attaches to the RS (zones 2–4), the goodput integral features multiple fold growth. Although some zones have improvement in multiple folds, those zones are too small (shown in Table 2). Therefore the overall performance improvement is not significant.

4.6 Energy savings

In this section, we extend our work to provide energy efficient multicast to BS. Additionally, let us assume the main cause of additional power consumption in BS is retransmit error bursts. We consider the 'average energy efficiency (AEE)' metric which is defined as the ratio of energy consumption for data transfer to the total energy consumption. This AEE metric has been first adopted in previous works such as [21] and [22]. Our goal is to maximise the AEE metric across all MSs receiving the same multicast stream in the coverage area. To achieve this goal, we assume that dense-enough MSs are receiving each multicast stream, thus multicast frames are copied to all RSs in the entire coverage area.

We evaluate and compare the energy savings resulted from our proposed scheme to that of the original scheme. In Fig. 8, we present the comparison between the two schemes when the channel quality and number of MS varies, respectively. The figures show that the proposed scheme with two strategies achieve high values for the AEE metric (close to 1) and remain significantly more efficient than the original scheme when the channel quality decreases. In addition, the results also show that the energy consumption increases when the number of MS increases. This directly reflects the fact that the channel quality and number of MS have both high impacts on energy efficiency, because our proposed scheme can reduce the frequency of retransmissions, which in turn reduces the total number of bursts needed. Table 6 also shows the AEE integral (i.e. CDF) from SNR = 5 to 25 in different number of MSs from $1(2^0)$ to $128(2^7)$. When using our proposed scheme, the energy consumptions are significantly improved in all expected AEEs.

The above simulation results demonstrate that the proposed CRC-based error-correction scheme is suitable for the multicasting in transparent mode MR networks because it reduces the PER and increases the goodput. These features enhance the transmission performance by reducing the number of retransmissions as well as consumption of the wireless resource. In particular, when an MS receives a multicast frame more than once, the error bit correction scheme is triggered in the first transmission. Moreover, if the MS selects the RS first attachment method, the impact area will increase to 70.67%, and the error-correction rate and energy efficiency will be optimal.

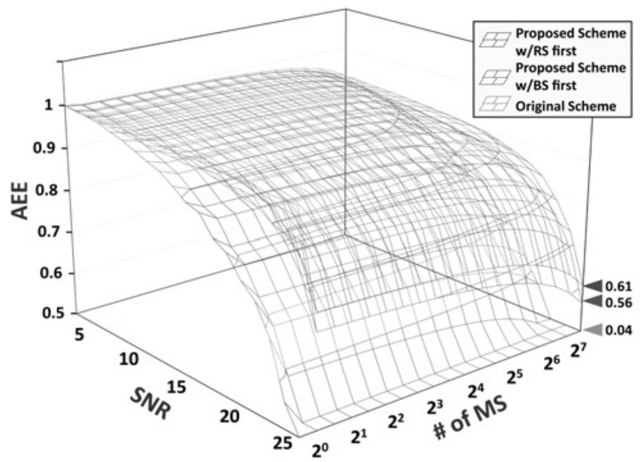

Fig. 8 *Energy efficiency against SNR and number of MS*

5 Concluding remarks

We presented a framework for reliable and energy-efficient multicasting in the transparent mode of WiMAX MR networks. We have considered the original CRC detection scheme and proposed a novel CRC-based error-correction

Table 6 AEE integral

Expected AEE	AEE integral, CDF			Enhancement, %	
	Original scheme	Proposed scheme (w/RS first)	Proposed scheme (w/BS first)	w/BS first	w/RS first
≥0.95	1.93	2.02	2.38	4	23
≥0.9	18.26	19.30	22.59	5	24
≥0.85	33.13	39.48	45.23	16	37
≥0.8	38.71	55.14	69.79	30	80
≥0.75	47.25	78.90	101.73	40	115
≥0.7	60.80	114.72	131.57	47	116
≥0.65	83.37	168.29	183.64	50	120
≥0.6	123.10	244.92	262.59	50	113
≥0.55	197.77	363.93	394.09	46	99
≥0.5	349.04	567.71	620.89	39	78

IET Commun., 2012, Vol. 6, Iss. 14, pp. 2169–2177
doi: 10.1049/iet-com.2011.0707

scheme. The proposed scheme separates the payload into segments and uses extra CRC calculator to compute the segmented FCSs individually. In the IEEE's work, the original CRC scheme is optional and only has limited error-detection capability in upper MAC layer. FCS occupies a few bits in a frame, but in our work, CRC is compulsory and all sub-FCSs are carried by padding space without requiring any extra bit. For the best error-correction capability, all transmissions must be padded as many s-FCSs as possible in cross layer. The simulation and numerical results demonstrate that our scheme achieves much better error-correction rate than the original CRC scheme, which uses the whole payload a and single CRC calculator to compute a single FCS directly.

In a multicast environment, if an MS receives the same frame from the BS and an RS, the bit error can be corrected during the first transmission, and if an MS only receives one frame from the BS, the bit error can be corrected in the first retransmission (i.e. the second transmission). Clearly, our approach can improve the throughput of WiMAX systems. The simulation results show that the PER improves significantly in a low transmission quality zone where the MSs have high packet error rates. Irrespective of the type of attachment method selected by the MS, the low-PER area (less than 10%) increases at least 2-fold; and in the best condition, the impacted area can be 3.5 times larger than under the original CRC scheme in the first transmission. Even if a frame must be retransmitted, our approach still achieves a superior error-correction performance.

The goodput of all zones also improves significantly under the proposed scheme. In zones where the MS attaches to the BS directly, the performance improves by 2–0.5 dB. For zones where the MS attaches to an RS, if the goodput decreases due to a reduced RS signal, the proposed scheme uses frames with extra CRCs from the BS to enhance its error-correction capability; therefore it can improve the goodput of MBS networks significantly. Using simulation, we showed that our algorithm achieves high energy efficiency. The scheme would be most useful in environments with extremely poor radio conditions. In addition, the scheme's error-detection capacity is slightly better than that of the original CRC scheme.

We believe that a few simple design modifications could yield a big improvement in the error detection, error correction and throughput of WiMAX networks. In principle, because the CRC circuit is inexpensive, the proposed scheme only slightly increase the network overhead, but the benefit would be substantial. Moreover, the proposed scheme is backward compatible with the legacy CRC error-detection scheme in WiMAX MR networks. Unlike the FEC approach, our proposed scheme does not increase the hardware complexity of the MAC significantly, and it does not require more bandwidth to carry the extra segmented CRC information.

The work in this paper can be extended in different directions. Apart from improving the performance of reliable OFDM-based wireless applications like Wi-Fi, MMDS, DAB, DVB-x, HDTV, UWB, 3GPP LTE and 3GPP LTE-A, or can be applied in several OFDM-based wired applications, such as xDSL, xPON, HiperLAN/2 and MoCA. Our approach facilitates wireless transmissions under very poor radio conditions, even if the FEC functions poorly. Moreover, it improves the energy efficiency and throughput of all types of modulation and/or coding rates.

6 References

1 Msadaa, I.C., Filali, F.: 'On the performance bounds of OFDM-based 802.16 broadband wireless networks'. IEEE Proc. Wireless Communications and Networking Conf. 2008 (WCNC 2008), 2008, pp. 1459–1464

2 van Nee, R.D.J., Prasad, R.: 'OFDM for wireless multimedia communications' (Artech House, 2000)

3 Terry, J., Heiskala, J.: 'OFDM wireless LANs: a theoretical and practical guide' (Sams, 2002)

4 IEEE Standard for Local and Metropolitan Area Networks Part 16: Air Interface for Fixed and Mobile Broadband Wireless Access Systems. Amendment for Physical and Medium Access Control Layers for Combined Fixed and Mobile Operation in Licensed Bands, IEEE Std 802.16e-2005, 2005

5 IEEE 802.16-2004, Part 16: Air Interface for Fixed Broadband Wireless Access Systems, IEEE Std 802.16-2004, 2004

6 Liu, H., Li, G.: 'OFDM-based broadband wireless networks: design and optimization' (John Wiley & Sons, 2005)

7 Liu, J., Li, J.: 'Parameter estimation and error reduction for OFDM-based WLANs', *IEEE Trans. Mob. Comput.*, 2004, **3**, (2), pp. 152–163

8 IEEE Standard for Local and Metropolitan Area Networks Part 16: Air Interface for Broadband Wireless Access Systems, Amendment 1: Multiple Relay Specification, IEEE Std 802.16j-2009, 2009

9 ITU, Recommendation G. 704. Synchronous frame structures used at 1544, 6312, 2048, 8448 and 44 736 kbit/s hierarchical levels, 1998

10 Mattes, T., Schiller, F., Mörwald, A., Pfahler, J., Honold, T.: 'Safety proof of combinations of CRC for industrial', *J. Appl. Comput. Sci.*, 2008, **16**, (1), pp. 15–32

11 Peterson, W., Weldon, E.J.: 'Error correcting codes' (MIT Press, 1996)

12 Hoymann, C., Puttner, M., Forkel, I.: 'The HIPERMAN standard–a performance analysis'. Proc. IST Mobile and Wireless Communication Summit, 2003

13 Hoymann, C., Puttner, M., Forkel, I.: 'Initial performance evaluation and analysis of the global OFDM metropolitan area network standard IEEE 802.16'. Proc. European Wireless Conf., 2004

14 Kuo, W.-H., Lee, j.-F.: 'Multicast routing scheme for recipient maximization in wireless relay networks', *IEEE Trans. Veh. Technol.*, 2010, **8**, (19), pp. 4002–4011

15 Kuo, W.-H., Lee, J.-F.: 'Multicast recipient maximization in IEEE 802.16j WiMAX relay networks', *IEEE Trans. Veh. Technol.*, 2010, **1**, pp. 335–343

16 Hoymann, C.: 'Analysis and performance evaluation of the OFDM based metropolitan area network IEEE 802.16', *Comput. Netw.*, 2005, **49**, (3), pp. 341–363

17 Genc, V., Murphy, S., Murphy, J., Nafaa, A.: 'System-level performance evaluation of multi-cell transparent mode relay 802.16j systems'. Proc. IEEE GLOBECOM 2009, 2009, pp. 1–7

18 Robinson, J., Knightly, E.: 'A performance study of deployment factors in wireless mesh networks'. Proc. IEEE INFOCOM, 2007, pp. 2054–2062

19 Shi, J., Fang, G., Sun, Y., Zhou, J., Li, Z., Dutkiewicz, E.: 'Improving mobile station energy efficiency in IEEE 802.16e WMAN by burst scheduling'. Proc. IEEE GLOBECOM'06, San Francisco, CA, USA, December 2006, pp. 1–5

20 Sharangi, S., Krishnamurti, R., Hefeeda, M.: 'Energy-efficient multicasting of scalable video streams over WiMAX networks', *IEEE Trans. Multimed.*, 2011, **13**, (1), pp. 102–115

21 Schiller, F., Mattes, T.: 'An efficient method to evaluate CRC-polynomials for safety-critical industrial communication', *J. Appl. Comput. Sci.*, 2006, **14**, (1), pp. 57–80

22 IEEE, IEEE 802.16 Broadband Wireless Access Working Group: 'Channel models for fixed wireless applications', June 2003